

pubs.acs.org/NanoLett Letter

How Exciton and Single Carriers Block the Excitonic Transition in Two-Dimensional Cadmium Chalcogenide Nanoplatelets

Qiuyang Li, Sheng He, and Tianquan Lian*



Cite This: Nano Lett. 2020, 20, 6162-6169



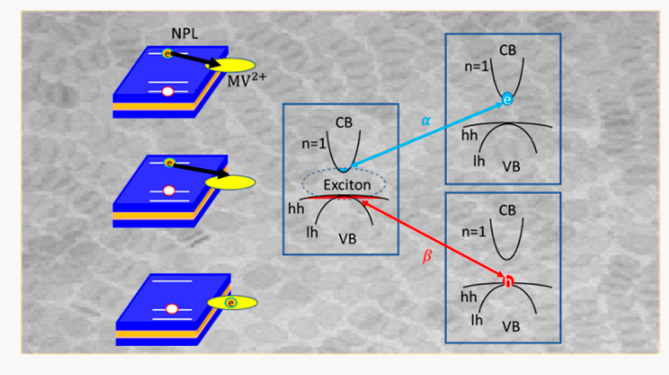
ACCESS

III Metrics & More

Article Recommendations

Supporting Information

ABSTRACT: Cadmium chalcogenide nanoplatelets (NPLs) possess unique properties and have shown great potential in lasing, light-emitting diodes, and photocatalytic applications. However, the exact natures of the band-edge exciton and single carrier (electron and hole) states remain unclear, even though they affect the key properties and applications of these materials. Herein, we study the contribution of a single carrier (electron or hole) state to phase space filling of single exciton states of cadmium chalcogenide NPLs. With pump fluence dependent TA study and selective electron removal, we determine that a single electron and hole states contribute 85% and 12%, respectively, to the blocking of the excitonic transition in CdSe/ZnS core/shell NPLs. These observations can be rationalized by a model of band-



edge exciton and single carrier states of 2D NPLs that differs significantly from that of quantum dots.

KEYWORDS: nanoplatelets, cadmium chalcogenide, 2D materials, transient absorption, exciton bleach

admium chalcogenide (CdX, X = Se, S, Te) twodimensional (2D) nanoplatelets (NPLs) and their heterostructures are of broad interests to the field of nanocrystals as they possess properties different from those of 0D quantum dots (QDs) and 1D nanorods (NRs), including narrow thickness distribution and uniform quantum confinement along the thickness direction, 1,2 high photoluminescent quantum yield (PLQY),^{3,4} long Auger lifetime,^{5–8} and superior charge transport and separation properties.^{9–15} They have demonstrated great potential applications in lasing, 16-22 light-emitting diodes, 23-25 and solar-to-hydrogen conversion. 10,26-28 Many properties of 2D NPLs, such as the optical gain mechanism and threshold, are determined by the structure and occupancies of band-edge energy levels in excitonic and single carrier (electron and hole) states. 19,21,29-33 One of the most convenient ways to probe these band-edge electronic structures is through the state filling effects of exciton or single carrier states on the band-edge exciton transitions, which leads to exciton bleach (XB) signals in transient absorption spectroscopy. The understanding of such effects has enabled the study of carrier dynamics,³⁴⁻ transfer kinetics, 27,37,39,40 and multiexciton annihilation 7,41in 0D, 1D, and 2D nanocrystals.

Despite the broad impacts and importance, how excitons and carriers block excitonic transitions in cadmium chalcogenide nanocrystals remains poorly understood. Early studies reported that the XB signal is dominated by conduction band (CB) edge electron state-filling in cadmium chalcogenide QDs, while valence band (VB) edge hole state-filling contributes

negligibly due mainly to the small level spacing and large degeneracy of valence band-edge hole levels. 44-46 This assignment is consistent with many TA studies of cadmium chalcogenide QD-acceptor complexes, in which the removal of the electron leads to complete recovery of the XB.⁴⁷⁻⁵⁰ However, a recent study of CdSe/CdS/ZnS core/shell/shell QDs shows that the VB hole blocks ~25% of the band-edge exciton transition.⁵¹ For 2D NPLs, our previous studies have shown that the XB signal of photoexcited CdX (X = Se, S, Te)NPLs is dominated by the state-filling of the CB edge electron with negligible hole contributions. 15,27,37 However, other studies have reported nonnegligible contributions of the VB hole to the XB signal. 52-54 Furthermore, for CsPbBr₃ perovskite 2D NPLs, both single electron and hole states have negligible contributions to the XB.55 Thus, how excitons and carriers contribute to the state filling of excitonic transitions in NPLs and how these effects depend on material properties remain open questions.

Here, we study the band-edge levels of core only CdSe and core/shell CdSe/ZnS NPLs by transient absorption (TA) spectroscopy. In CdSe/ZnS core/shell NPLs, we determine

Received: June 18, 2020 Revised: July 21, 2020 Published: July 22, 2020





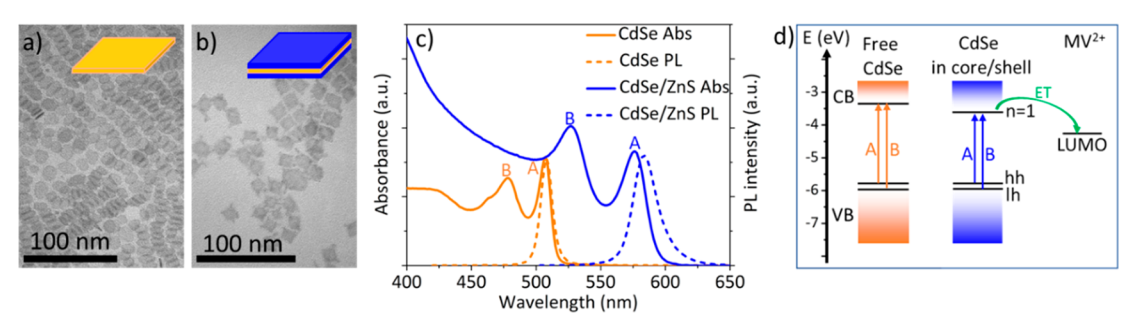


Figure 1. TEM images of (a) 4 ML CdSe NPLs and (b) CdSe/ZnS core/shell NPLs. Insets of (a) and (b): schemes of core-only NPLs and core/shell NPLs. (c) Absorption (solid lines) and photoluminescence (dashed lines) spectra of 4 ML CdSe and CdSe/ZnS core/shell NPLs. (d) Schematic energy levels (vs vacuum) of 4 ML CdSe NPLs, 4 ML CdSe/ZnS core/shell NPLs, and the reduction potential (LUMO) of methyl viologen (MV²⁺). CB: conduction band. VB: valence band. hh: heavy hole. lh: light hole levels. ET: electron transfer.

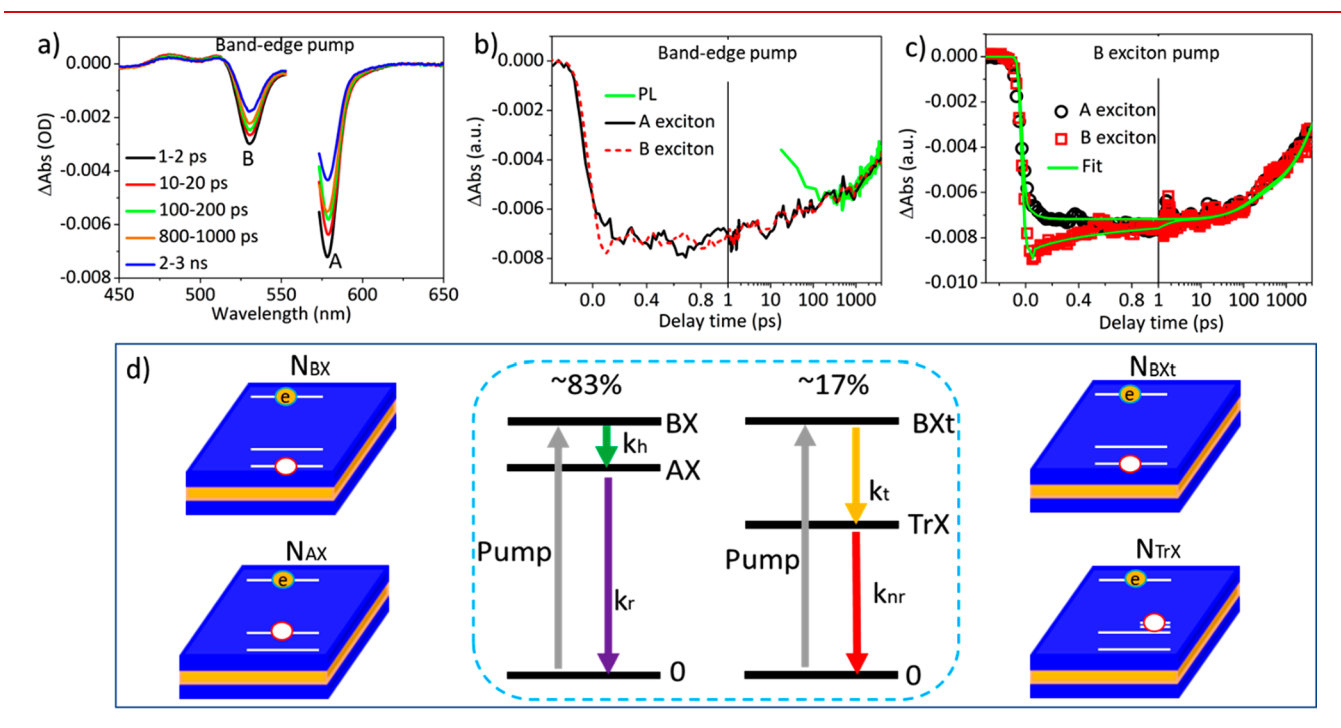


Figure 2. (a) TA spectra of CdSe/ZnS core/shell NPLs under band-edge pump (~565 nm) at indicated delay times. (b) Comparison of A and B exciton bleach kinetics and PL decay kinetics of CdSe/ZnS core/shell NPLs at band-edge pump. (c) Comparison of A and B exciton bleach kinetics of CdSe/ZnS core/shell NPLs at B exciton pump (~520 nm). Solid lines are the fits. (d) Schemes of different species that contribute to XB of CdSe/ZnS core/shell NPLs. Middle panel: species decay pathways in CdS/ZnS core/shell NPLs without (left column) and with (right column) hole trap states at B exciton pump (520 nm) in state representation.

the contribution of the single electron state to the exciton transition by preparing different initial exciton states. By selectively removing the electron from NPLs using methylviologen as an electron acceptor, we also determine how the remaining single VB hole contributes to the XB signal. Moreover, we investigate how hole trapping affects the XB signal by comparing high PLQY CdSe/ZnS core/shell NPLs and low PLQY CdSe and CdS NPLs. These results lead to unambiguous determination of the contribution of a single electron, hole, and exciton states to the XB signal. To explain these observations, a model for band edge exciton and single carrier states are proposed.

CdSe and CdSe/ZnS core/shell NPLs were synthesized following reported procedures. The synthesis details are shown in Supporting Information (SI) S1. CdSe NPLs with 4 monolayer (ML) thickness show a truncated rectangular shape (Figure 1a) with average length and width of 12.8 ± 1.6 and 8.4 ± 1.2 nm, respectively (Figure S1a,b). CdSe/ZnS core/

shell NPLs were prepared by coating ZnS shells on both basal planes of CdSe NPLs, which show a rectangular shape (Figure 1b) with an average length and width of 14.8 \pm 1.7 and 11.7 \pm 1.1 nm, respectively (Figure S1c,d). Figure 1c shows the absorption and photoluminescence (PL) spectra of CdSe and CdSe/ZnS core/shell NPLs. For CdSe NPLs, the absorption peaks at ~510 and ~480 nm correspond to the transitions to the CB edge electron from the heavy hole (hh) (A exciton) and from the light hole (lh) (B exciton), respectively (Figure 1d). These peaks are shifted to ~580 and ~530 nm in CdSe/ ZnS core/shell NPLs. 3,56 PL spectra of CdSe and CdSe/ZnS NPLs show a single emission peak at ~511 and ~585 nm, respectively, corresponding to their band-edge (A exciton) emission. The PLQY is determined to be ~12% and ~83% for CdSe and CdSe/ZnS core/shell NPLs, respectively, indicating that trap mediated nonradiative recombination is the dominant decay pathway for of excitons in ~88% core-only CdSe NPLs and ~17% core/shell NPLs. Because trapped excitons in

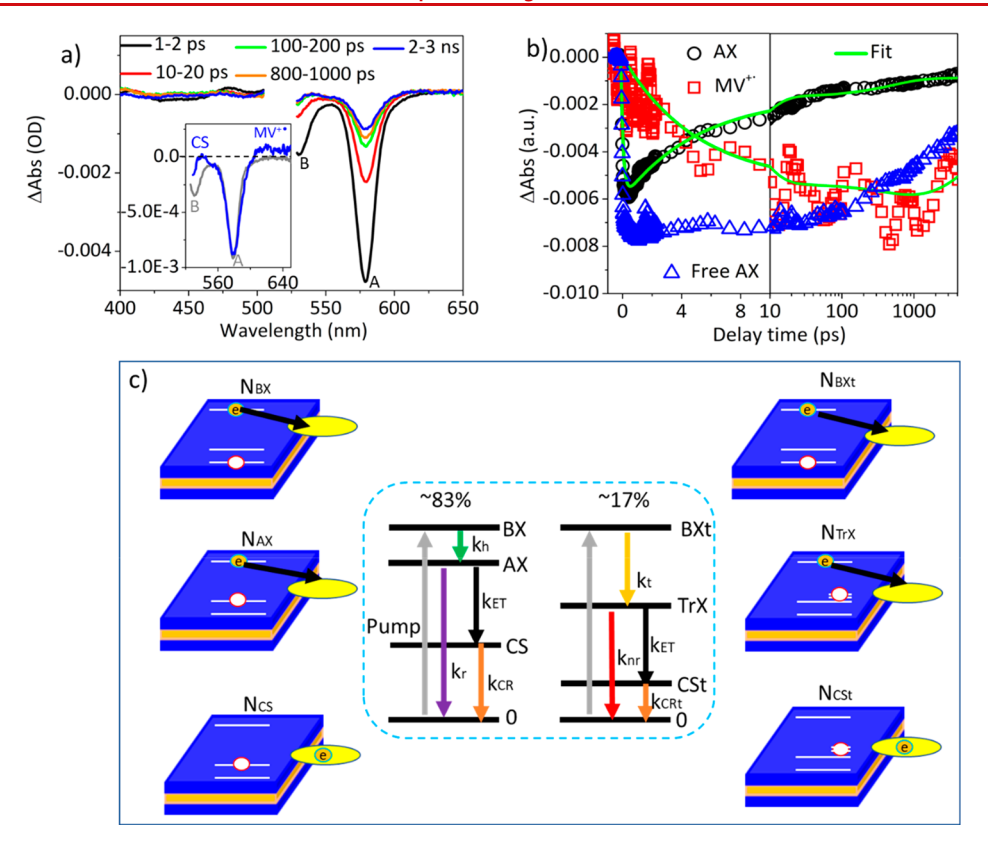


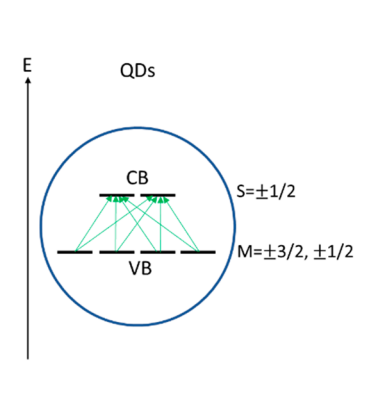
Figure 3. (a) TA spectra of CdSe/ZnS NPL $-MV^{2+}$ complexes under B exciton pump (\sim 520 nm) at indicated delay times. Inset: comparison of TA spectra at 2-3 ns of CdSe/ZnS NPL $-MV^{2+}$ complexes (blue) and free CdSe/ZnS NPLs (gray). The amplitude of free CdSe/ZnS NPLs (gray) is divided by a factor of 4. (b) Kinetics of A exciton bleach (black circles) and reduced methyl viologen radicals (MV^{+*} , red squares) of CdSe/ZnS NPL $-MV^{2+}$ complexes, and A exciton bleach of free CdSe/ZnS NPLs (blue triangles). Green lines are the fits according to the ET model shown in SI S4. (c) Schemes of different species that contribute to XB of NPL $-MV^{2+}$ complexes. Middle panel: species decay pathways in CdS/ZnS core/shell NPL $-MV^{2+}$ complexes without (left column) and with (right column) hole trap states in NPLs at B exciton pump (520 nm) in state representation.

cadmium chalcogenide NPLs are dominated by hole trapping, ^{14,27,37,52,53,57} these NPLs are ideal models to investigate the effect of hole trapping on XB signals.

To study how excitons block the excitonic transitions in 2D NPLs, we compare TA spectra measured with excitation at A and B excitonic transitions for CdSe/ZnS core/shell NPLs at room temperature. The excitation fluence was kept low (~2 μ J/cm²) and the fractional bleach, the ratio of transient absorption bleach amplitude (Figure 2a) to sample absorbance (Figure S4a), at the A exciton bleach was estimated to be 4.4%. Under this condition, single exciton states dominate the observed signal. We first measured the TA spectra of CdSe/ ZnS core/shell NPLs with excitation at their band-edge (~565 nm) so that only the single A exciton states, with an electron at the CB edge and a hh at the VB edge, are excited. These TA spectra (Figure 2a) show sharp A and B exciton bleach signals at ~580 and ~530 nm, respectively, resulting from the blockage of A and B exciton transitions by the band-edge exciton, stimulated emission, and photoinduced absorption. In this case, the A exciton bleach kinetics is determined by the state-filling of both the CB electron and VB hole while the B exciton bleach kinetics is only determined by the state-filling of the CB electron. Figure 2b shows that the A and B exciton bleach kinetics are identical and agree with the PL decay kinetics, indicating that both the XB recovery and PL decays probe the band-edge exciton recombination process. Note that the PL kinetics starts after 120 ps because of the limited

instrument response time of the time-resolved PL measurement (\sim 110 ps).

To quantify how a single electron blocks the excitonic transition, we measured the TA spectra of CdSe/ZnS core/ shell NPLs with excitation at ~520 nm, which directly excites the B exciton state (with an electron at the CB edge and a lh in the VB). In this case, the hole will relax from the lh to the hh level after excitation. Figure 2c shows that the normalized A and B exciton kinetics are identical after 2 ps but deviate from each other at <2 ps: B exciton bleach shows a fast decay while A exciton bleach shows a corresponding growth. This initial process within 2 ps indicates that the relaxation of the VB hole from the lh to hh level can be observed through their contribution to the A and B exciton bleach signals, similar to previous reports on cadmium chalcogenide NPLs⁵³ and QDs. 51 We fit both the A and B exciton kinetics (Figure 2c) with a model accounting for the contribution to the XB from different species (Figure 2d). Because the PLQY of CdSe/ZnS NPLs is ~83%, and the hole trapping (in subps) in NPLs is much faster than exciton radiative recombination (in ns), 37,52,53 we consider two species in solution: (1) ~83% NPLs with no hole traps, in which the long-lived A exciton (AX) state is generated from the initial B exciton (BX) after hole relaxation; (2) \sim 17% NPLs with hole traps, in which the long-lived trapped exciton state (TrX, with a CB edge electron and a trapped hole) is generated from the B exciton state (BXt) by rapid hole trapping to surface states within the gap



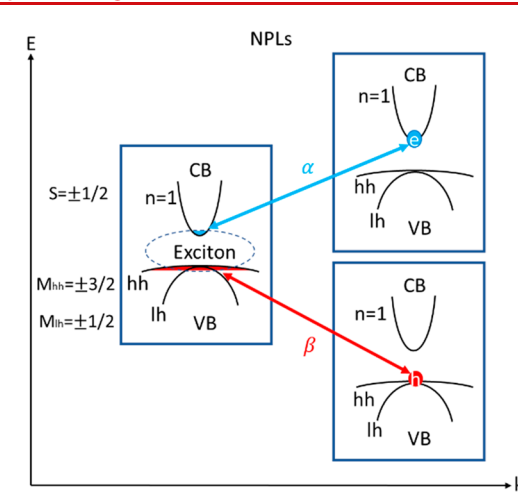


Figure 4. Left panel: scheme of possible transitions between band-edge electron and hole degenerated levels in cadmium chalcogenide QDs. Green lines represent the transitions. Right panel: schemes of band structure of cadmium chalcogenide NPLs and the occupation of an exciton, a single electron, and a single hole at the NPL band-edge, respectively. S and M (M_{hh} and M_{lh}) are possible spin projections for CB electron levels and total angular momentum projections for VB hole levels (hh and lh band), respectively.

region.⁵⁸ The XB intensity is determined by the population and contributions of these species to the XB. We assume that a single electron blocks an excitonic transition by a factor of α less than an exciton. These species undergo radiative (for ~83% NPLs without trap) or nonradiative decay (for ~17% NPLs with hole traps) after B exciton excitation (middle panel of Figure 2d). The details of the model and fitting procedure are shown in SI S4. The best fit (Figure 2c) yields a hole relaxation time (τ_h) and trapping time (τ_t) of 803 \pm 8 fs and 169 \pm 5 fs, respectively, and α of 85 \pm 2%. The subpicosecond hole trapping time extracted here is consistent with previously reported values, 37,52,53 but the extracted α value is larger than that reported in CdSe/CdS core/shell NPLs (~64%).52 The reason for this deviation remains unclear, it may be attributed to the different shell materials, shell thickness, lateral dimension, and sample quality. Although the PLQY of CdSe/CdS core/shell NPLs is not reported in ref 52, it is known to depend on both shell material (CdS vs CdZnS)^{4,56} and shell thickness.³ Different PLOYs can be caused by different carrier trapping and exciton transition strengths. The latter depends on the band-edge levels involved in the exciton transitions, ⁵⁹ which determine α as we will discuss below (Figure 4). A similar decrease of XB amplitude by hole removal was observed previously for CdSe NPLs, but it was attributed to the spectrum shift caused by hole removal rather than a change in hole state filling contributions.⁵⁴

To investigate how a single VB hole blocks the excitonic transition, we selectively transfer the CB electron from CdSe/ ZnS core/shell NPLs to the methyl viologen (MV2+) in NPL- MV^{2+} complexes. The reduction potential of MV^{2+} (-4.26 eV vs vacuum) 60 is lower than the CB edge of CdSe NPLs (-3.37 eV) and CdSe/ZnS NPLs (-3.62 eV), as shown in Figure 1d (see SI S3 for details). The reduced methyl viologen (MV+* radicals) has a broad absorption at ~600 nm. 61 We compare free NPL and NPL-MV2+ samples with the same NPL concentrations, which leads to the same optical densities at the excitation wavelength (Figure S4a-c) and the same numbers of absorbed excitation photons and average numbers of excitons per NPL under the same excitation fluence. The PL of all NPL-MV²⁺ complexes (Figure S4d-f) are completely quenched, indicating complete quenching of NPL excitons by electron transfer (ET) to MV²⁺. The TA spectra and kinetics

(Figure 3a,b) of CdSe/ZnS core/shell NPL-MV²⁺ complexes measured with B exciton excitation (~520 nm) show the formation of MV+* signal at 600-650 nm and the corresponding decay of XB, confirming ET from the NPL to MV²⁺. When ET is completed at 2-3 ns, ^{28,37,62,63} the TA spectra (inset of Figure 3a) show a derivative feature around the B exciton band (~530 nm). It is attributed to the chargeseparated (CS) state, with the electron transferred to MV+* and hole remaining in NPLs, which shifts the B exciton transition energy,³⁷ similar to cadmium chalcogenide QDs and nanorods.^{36,61,64} This derivative feature can be more clearly seen in the TA spectra at 400 nm excitation (Figure S5b). However, the A exciton bleach signal remains at 2-3 ns, which is attributed to the VB hole remained at hh level, which blocks the A exciton transition. Although there should also be a CS signal at the A exciton transition, it is estimated to be much smaller than the electron and hole state filling signals (see SI \$5 for details) and is not observed.

To quantify how a single hole contributes to the XB, we fit the A exciton bleach and MV^{+*} kinetics in CdSe/CdS core/shell NPL-MV²⁺ complexes using the model shown in Figure 3c and eqs S16-S31 in the Supporting Information. In addition to the intra-NPL decay processes of free NPLs (Figure 2d), this model contains the CS state (CS and CSt for NPLs without and with hole traps, respectively) formed by ET from AX or TrX to MV²⁺ and its decay by charge recombination. We assume that a single hole in the hh level in the CS state blocks the A exciton transition by a factor β smaller than that of an A exciton (see SI S4 for fitting details). The best fit (Figure 3b) gives ET times of 4.15 \pm 0.91 ps (86 \pm 2%) and 813 \pm 108 ps (14 \pm 2%) and β value of 12 \pm 3%. This value is smaller than reported value for CdSe QDs (~30%).⁵¹

TA studies of CdSe NPL-MV²⁺ and CdS NPL-MV²⁺ complexes, prepared with low PLQY CdSe (~12%) and CdS (<1%) NPLs, show a lack of hole state filling signals at long delay time. The hole state filling signal amplitude in CdSe NPLs is estimated to be <1.8% because of ultrafast hole trapping (see SI S6 for details) and this finding also explains the negligible hole contribution to XB bleach signal in core-only CdSe and CdS NPLs reported previously.^{7,14,27,33,37}

How single carriers (electron and hole) block the excitonic transition compared to an exciton in NPLs is determined by the nature of single exciton and carrier states. 65-68 In a recent model of CdSe QDs, it is assumed that band-edge excitons involve electron and hole levels with 2- and 4-fold degeneracies, respectively (left panel of Figure 4), and the excitonic transition between these levels have the same transition strength.⁵¹ This model assumes the same sets of discrete states in exciton and single electron (or hole) states, which is likely not applicable for 2D NPLs due to two reasons. (1) 2D NPLs are only quantum confined along the thickness (z) direction and there is a continuum of free carrier states with well-defined momentum along the basal plane (in the x-ydirection) of NPLs. Thus, in addition to the discrete states resulted from the quantum confinement effect, the continuum of k-states should also be considered. (2) The dielectric confinement effect in 2D nanostructures leads to a larger exciton binding energy (~100-200 meV)^{1,69} than QDs. The wave function of excitons is a superposition of many continuous band-edge free electron and hole states. 70,71

Here, we propose a qualitative model to explain the transient exciton bleach signal of 2D NPLs (right panel of Figure 4) following the seminal work of Schmitt-Rink and co-workers. In this model, an exciton, electron or hole can block the exciton transition because of the phase space filling effect. The 2D exciton is described by the 2D hydrogen model, 65–68 and the free electron and hole are described by a free carrier gas. The extent of phase space filling for each particle is described by eq 1.

$$\frac{\delta F_{\rm p}}{F} = -\frac{N}{N_{\rm S}} = -\sum_{\mathbf{k}} f_{\rm p}(\mathbf{k}) \frac{U_{\rm 1S}(\mathbf{k})}{U_{\rm 1S}(\mathbf{r}=0)}$$
(1)

In eq 1, F and δF_p are the total transition strength for 1S exciton state and the blockage of the 1S exciton transition strength by a single particle p (p = exciton, electron or hole), respectively. $U_{1S}(\mathbf{r})$ is the 1S exciton wave function of the 2D hydrogen model, 65 and $U_{1S}(\mathbf{k})$ is the Fourier transform of $U_{1S}(\mathbf{r})$. \mathbf{r} is the relative distance between electron and hole, and **k** is momentum. $f_n(\mathbf{k})$ is the probability of finding the particle in that k-state. N is the particle density and Ns is the saturation particle density. $1/N_S$ can also be interpreted as the area blocked out by the presence of a particle and reflects the extent of space filling by the particle. Within this phase-space filling model, the $1/N_{\rm S}$ values are $(32/7)\pi a_{\rm 2D}^2$, $0.87*8\pi a_{\rm 2D}^2$, and $0.13*8\pi a_{2D}^{2}$ for an exciton, electron, and hole, respectively.⁶⁶ Here we have assumed the low temperature limit, $k_{\rm B} {\rm T} \ll E_{\rm 1S}$, because of strong exciton binding in NPLs ($E_{1S} \sim 100-200$ meV)^{1,69} This model predicts α = 1.52, β = 0.23, and α/β = 6.92. The predicted values of α and β according to this model deviate from the measured values. One possible reason is that this model does not consider the contribution of stimulated emission from the exciton state, which further increases the exciton bleach caused by the presence of an exciton. This effect does not exist for an electron or hole state. Furthermore, this model assumes that the exciton state can be described by a 2D hydrogenic model, which is an approximation for NPLs with finite thickness. Therefore, more comprehensive theoretical studies are required to explicitly model the nature of wave functions in the exciton and single carrier states and provide quantitative estimations for α and β . Interestingly, the predicted ratio of these values is in excellent agreement of the measured ratio of 7.08. This ratio is only determined by the

ratio of electron and hole effective masses and is independent of the model of the exciton. This agreement supports the notion that electron and hole state filling effects reflect the different densities of states of their in-plane motions in these NPLs.

It is worth noting that, in 2D NPLs, the hh band splits from the lh band away from the Γ point and has two possible total angular momentum projections $(\pm 3/2)$, so that each k-state in the hh band is doubly degenerate, the same as the k-states in the lowest electron band. Although the degeneracy of band-edge hole levels in 2D NPLs is smaller than that for QDs and should increase its contribution to the exciton state filling, this is not observed. Instead, the presence of the large density of free hole states along the x-y plane reduces the state filling effect of a single hole state, differing significantly from that of QDs. This model predicts that as the lateral size of the NPL decreases to reach the quantum confinement regime, bandedge states will become more quantized and α and β values approach those for QDs.

According to our model, the sum of α and β is not necessarily unity, unlike the proposed model for cadmium chalcogenide QDs. 51 α and β values are different because the band-edge levels involved in electron and hole states have different overlaps with those involved in the exciton state due to different energy level spacing along the confined dimension and dispersion relationships of free in-plane carrier motions. This model can also explain our previous observation that in CsPbBr₃ perovskite 2D NPLs single carriers (either electron or hole) have negligible contributions to the XB, and only band-edge excitons result in an XB signal. This indicates that the exciton state in CsPbBr₃ NPLs may involve many CB and VB band levels that single electron or hole states have negligibly small overlaps with the exciton state.

In summary, we provide quantitative experimental evidence of how excitons and single carriers (electron and hole) block the excitonic transition of 2D cadmium chalcogenide NPLs via TA spectroscopy. By comparing selective excitation of A and B exciton states, we show that a single CB electron state blocks ~85% of the A exciton transition. By selective ET from NPLs to MV²⁺, we determine that a single VB edge hole state blocks only ~12% of the A exciton transition. We show that hole contributions to XB are negligible in low PLQY CdSe and CdS NPLs because of rapid hole trapping. The contributions of single carrier states to the XB are determined by the wave function overlap of the single carrier states with the exciton state according to a phase space filling model. Within this model the denser valence states of in-plane free hole motion accounts for the relatively small contribution of a single hole state to the XB compared to a single electron state. We believe that this model provides a framework for understanding state filling effects in other 2D NPLs systems, such as CsPbBr₃ NPLs, and even 1D nanocrystals. Our findings contribute to not only the fundamental understanding of optical transitions and carrier dynamics of NPLs but also the rational design and performance improvement of NPL based optoelectrical system.

METHODS

Sample Synthesis. The colloidal CdSe, CdSe/ZnS, and CdS NPLs were synthesized following the literatures with slight modifications. ^{1,3,72} Detailed synthesis procedures are shown in the SI S1.

Experimental Setup. Femtoseconds TA measurements were carried out by a regeneratively amplified Ti:sapphire laser

system (Coherent Astrella, 800 nm, 35 fs, 5.5 mJ/pulse, and 1 kHz repetition rate). The TA signals were collected and analyzed by the Helios system (Ultrafast Systems LLC). PL measurements were conducted with FluoroMax-3 spectro-fluorometer of HORIBA Scientific. Details of the experimental setup and optical characterizations of NPLs are shown in SI S2.

■ ASSOCIATED CONTENT

Supporting Information

The Supporting Information is available free of charge at https://pubs.acs.org/doi/10.1021/acs.nanolett.0c02461.

Synthesis procedures, length and width histograms, TEM image, absorption, PL, and TA spectra, exciton bleach kinetics, fitting parameters, and estimation details (PDF)

AUTHOR INFORMATION

Corresponding Author

Tianquan Lian — Department of Chemistry, Emory University, Atlanta, Georgia 30322, United States; ● orcid.org/0000-0002-8351-3690; Email: tlian@emory.edu

Authors

Qiuyang Li — Department of Chemistry, Emory University, Atlanta, Georgia 30322, United States; orcid.org/0000-0002-8192-3960

Sheng He – Department of Chemistry, Emory University, Atlanta, Georgia 30322, United States

Complete contact information is available at: https://pubs.acs.org/10.1021/acs.nanolett.0c02461

Notes

The authors declare no competing financial interest.

ACKNOWLEDGMENTS

This work is supported by the National Science Foundation (CHE-1709182, CHE-1726536, and CHE-2004080 to T. L.).

REFERENCES

- (1) Ithurria, S.; Tessier, M. D.; Mahler, B.; Lobo, R. P. S. M.; Dubertret, B.; Efros, A. Colloidal Nanoplatelets with Two-Dimensional Electronic Structure. *Nat. Mater.* **2011**, *10*, 936–941.
- (2) Tessier, M. D.; Javaux, C.; Maksimovic, I.; Loriette, V.; Dubertret, B. Spectroscopy of Single CdSe Nanoplatelets. ACS Nano 2012, 6, 6751–6758.
- (3) Altintas, Y.; Quliyeva, U.; Gungor, K.; Erdem, O.; Kelestemur, Y.; Mutlugun, E.; Kovalenko, M. V.; Demir, H. V. Highly Stable, near-Unity Efficiency Atomically Flat Semiconductor Nanocrystals of CdSe/ZnS Hetero-Nanoplatelets Enabled by ZnS-Shell Hot-Injection Growth. *Small* **2019**, *15*, 1804854.
- (4) Tessier, M. D.; Mahler, B.; Nadal, B.; Heuclin, H.; Pedetti, S.; Dubertret, B. Spectroscopy of Colloidal Semiconductor Core/Shell Nanoplatelets with High Quantum Yield. *Nano Lett.* **2013**, *13*, 3321–3328.
- (5) Kunneman, L. T.; Tessier, M. D.; Heuclin, H.; Dubertret, B.; Aulin, Y. V.; Grozema, F. C.; Schins, J. M.; Siebbeles, L. D. A. Bimolecular Auger Recombination of Electron-Hole Pairs in Two-Dimensional CdSe and CdSe/CdZnS Core/Shell Nanoplatelets. *J. Phys. Chem. Lett.* **2013**, *4*, 3574–3578.
- (6) Baghani, E.; O'Leary, S. K.; Fedin, I.; Talapin, D. V.; Pelton, M. Auger-Limited Carrier Recombination and Relaxation in CdSe Colloidal Quantum Wells. *J. Phys. Chem. Lett.* **2015**, *6*, 1032–1036.

- (7) Li, Q.; Lian, T. Area- and Thickness-Dependent Biexciton Auger Recombination in Colloidal CdSe Nanoplatelets: Breaking the "Universal Volume Scaling Law. *Nano Lett.* **2017**, *17*, 3152–3158.
- (8) Pelton, M.; Andrews, J. J.; Fedin, I.; Talapin, D. V.; Leng, H.; O'Leary, S. K. Nonmonotonic Dependence of Auger Recombination Rate on Shell Thickness for CdSe/CdS Core/Shell Nanoplatelets. *Nano Lett.* **2017**, *17*, 6900–6906.
- (9) Rowland, C. E.; Fedin, I.; Zhang, H.; Gray, S. K.; Govorov, A. O.; Talapin, D. V.; Schaller, R. D. Picosecond Energy Transfer and Multiexciton Transfer Outpaces Auger Recombination in Binary CdSe Nanoplatelet Solids. *Nat. Mater.* **2015**, *14*, 484–489.
- (10) Zhukovskyi, M.; Tongying, P.; Yashan, H.; Wang, Y.; Kuno, M. Efficient Photocatalytic Hydrogen Generation from Ni Nanoparticle Decorated Cds Nanosheets. *ACS Catal.* **2015**, *5*, 6615–6623.
- (11) Pedetti, S.; Ithurria, S.; Heuclin, H.; Patriarche, G.; Dubertret, B. Type-II CdSe/CdTe Core/Crown Semiconductor Nanoplatelets. *J. Am. Chem. Soc.* **2014**, *136*, 16430–16438.
- (12) Tessier, M. D.; Spinicelli, P.; Dupont, D.; Patriarche, G.; Ithurria, S.; Dubertret, B. Efficient Exciton Concentrators Built from Colloidal Core/Crown CdSe/CdS Semiconductor Nanoplatelets. *Nano Lett.* **2014**, *14*, 207–213.
- (13) Li, Q.; Zhou, B.; McBride, J. R.; Lian, T. Efficient Diffusive Transport of Hot and Cold Excitons in Colloidal Type II Cdse/Cdte Core/Crown Nanoplatelet Heterostructures. *ACS Energy Letters* **2017**, *2*, 174–181.
- (14) Li, Q.; Wu, K.; Chen, J.; Chen, Z.; McBride, J. R.; Lian, T. Size-Independent Exciton Localization Efficiency in Colloidal CdSe/CdS Core/Crown Nanosheet Type-I Heterostructures. *ACS Nano* **2016**, *10*, 3843–3851.
- (15) Wu, K.; Li, Q.; Jia, Y.; McBride, J. R.; Xie, Z.-X.; Lian, T. Efficient and Ultrafast Formation of Long-Lived Charge-Transfer Exciton State in Atomically Thin Cadmium Selenide/Cadmium Telluride Type-II Heteronanosheets. ACS Nano 2015, 9, 961–968.
- (16) Grim, J. Q.; Christodoulou, S.; Di Stasio, F.; Krahne, R.; Cingolani, R.; Manna, L.; Moreels, I. Continuous-Wave Biexciton Lasing at Room Temperature Using Solution-Processed Quantum Wells. *Nat. Nanotechnol.* **2014**, *9*, 891–895.
- (17) Guzelturk, B.; Kelestemur, Y.; Olutas, M.; Delikanli, S.; Demir, H. V. Amplified Spontaneous Emission and Lasing in Colloidal Nanoplatelets. *ACS Nano* **2014**, *8*, 6599–6605.
- (18) She, C. X.; Fedin, I.; Dolzhnikov, D. S.; Demortiere, A.; Schaller, R. D.; Pelton, M.; Talapin, D. V. Low-Threshold Stimulated Emission Using Colloidal Quantum Wells. *Nano Lett.* **2014**, *14*, 2772–2777.
- (19) Li, Q.; Xu, Z.; McBride, J. R.; Lian, T. Low Threshold Multiexciton Optical Gain in Colloidal CdSe/CdTe Core/Crown Type-II Nanoplatelet Heterostructures. *ACS Nano* **2017**, *11*, 2545–2553.
- (20) Diroll, B. T.; Talapin, D. V.; Schaller, R. D. Violet-to-Blue Gain and Lasing from Colloidal Cds Nanoplatelets: Low-Threshold Stimulated Emission Despite Low Photoluminescence Quantum Yield. ACS Photonics 2017, 4, 576–583.
- (21) Tomar, R.; Kulkarni, A.; Chen, K.; Singh, S.; Van Thourhout, D.; Hodgkiss, J. M.; Siebbeles, L. D. A.; Hens, Z.; Geiregat, P. Charge Carrier Cooling Bottleneck Opens up Nonexcitonic Gain Mechanisms in Colloidal CdSe Quantum Wells. *J. Phys. Chem. C* **2019**, *123*, 9640–9650.
- (22) Geiregat, P.; Tomar, R.; Chen, K.; Singh, S.; Hodgkiss, J. M.; Hens, Z. Thermodynamic Equilibrium between Excitons and Excitonic Molecules Dictates Optical Gain in Colloidal CdSe Quantum Wells. *J. Phys. Chem. Lett.* **2019**, *10*, 3637–3644.
- (23) Liu, B.; Delikanli, S.; Gao, Y.; Dede, D.; Gungor, K.; Demir, H. V. Nanocrystal Light-Emitting Diodes Based on Type II Nanoplatelets. *Nano Energy* **2018**, 47, 115–122.
- (24) Giovanella, U.; Pasini, M.; Lorenzon, M.; Galeotti, F.; Lucchi, C.; Meinardi, F.; Luzzati, S.; Dubertret, B.; Brovelli, S. Efficient Solution-Processed Nanoplatelet-Based Light-Emitting Diodes with High Operational Stability in Air. *Nano Lett.* **2018**, *18*, 3441–3448.

- (25) Selyukov, A. S.; Vitukhnovskii, A. G.; Lebedev, V. S.; Vashchenko, A. A.; Vasiliev, R. B.; Sokolikova, M. S. Electroluminescence of Colloidal Quasi-Two-Dimensional Semiconducting Cdse Nanostructures in a Hybrid Light-Emitting Diode. *J. Exp. Theor. Phys.* **2015**, *120*, 595–606.
- (26) Naskar, S.; Lübkemann, F.; Hamid, S.; Freytag, A.; Wolf, A.; Koch, J.; Ivanova, I.; Pfnür, H.; Dorfs, D.; Bahnemann, D. W.; Bigall, N. C. Synthesis of Ternary and Quaternary Au and Pt Decorated CdSe/CdS Heteronanoplatelets with Controllable Morphology. *Adv. Funct. Mater.* **2017**, *27*, 1604685.
- (27) Li, Q.; Zhao, F.; Qu, C.; Shang, Q.; Xu, Z.; Yu, L.; McBride, J. R.; Lian, T. Two-Dimensional Morphology Enhances Light-Driven H₂ Generation Efficiency in CdS Nanoplatelet-Pt Heterostructures. *J. Am. Chem. Soc.* **2018**, *140*, 11726–11734.
- (28) Li, Q.; Lian, T. Exciton Dissociation Dynamics and Light-Driven H₂ Generation in Colloidal 2D Cadmium Chalcogenide Nanoplatelet Heterostructures. *Nano Res.* **2018**, *11*, 3031–3049.
- (29) Klimov, V. I.; Ivanov, S. A.; Nanda, J.; Achermann, M.; Bezel, I.; McGuire, J. A.; Piryatinski, A. Single-Exciton Optical Gain in Semiconductor Nanocrystals. *Nature* **2007**, *447*, 441–446.
- (30) Wu, K.; Park, Y.-S.; Lim, J.; Klimov, V. I. Towards Zero-Threshold Optical Gain Using Charged Semiconductor Quantum Dots. *Nat. Nanotechnol.* **2017**, *12*, 1140–1147.
- (31) Guzelturk, B.; Kelestemur, Y.; Olutas, M.; Li, Q.; Lian, T.; Demir, H. V. High-Efficiency Optical Gain in Type-II Semiconductor Nanocrystals of Alloyed Colloidal Quantum Wells. *J. Phys. Chem. Lett.* **2017**, *8*, 5317–5324.
- (32) Li, Q.; Lian, T. A Model for Optical Gain in Colloidal Nanoplatelets. *Chemical Science* **2018**, *9*, 728–734.
- (33) Li, Q.; Liu, Q.; Schaller, R. D.; Lian, T. Reducing the Optical Gain Threshold in Two-Dimensional CdSe Nanoplatelets by the Giant Oscillator Strength Transition Effect. *J. Phys. Chem. Lett.* **2019**, 10, 1624–1632.
- (34) Norris, D. J.; Sacra, A.; Murray, C. B.; Bawendi, M. G. Measurement of the Size Dependent Hole Spectrum in CdSe Quantum Dots. *Phys. Rev. Lett.* **1994**, *72*, 2612.
- (35) Klimov, V. I.; McBranch, D. W.; Leatherdale, C. A.; Bawendi, M. G. Electron and Hole Relaxation Pathways in Semiconductor Quantum Dots. *Phys. Rev. B: Condens. Matter Mater. Phys.* **1999**, *60*, 13740–13749.
- (36) Wu, K. F.; Zhu, H. M.; Liu, Z.; Rodriguez-Cordoba, W.; Lian, T. Q. Ultrafast Charge Separation and Long-Lived Charge Separated State in Photocatalytic CdS-Pt Nanorod Heterostructures. *J. Am. Chem. Soc.* **2012**, *134*, 10337–10340.
- (37) Wu, K.; Li, Q.; Du, Y.; Chen, Z.; Lian, T. Ultrafast Exciton Quenching by Energy and Electron Transfer in Colloidal CdSe Nanosheet-Pt Heterostructures. *Chemical Science* **2015**, *6*, 1049–1054.
- (38) Morgan, D. P.; Kelley, D. F. Exciton Localization and Radiative Lifetimes in CdSe Nanoplatelets. *J. Phys. Chem. C* **2019**, *123*, 18665–18675.
- (39) Zhu, H. M.; Lian, T. Q. Wavefunction Engineering in Quantum Confined Semiconductor Nanoheterostructures for Efficient Charge Separation and Solar Energy Conversion. *Energy Environ. Sci.* **2012**, *5*, 9406–9418.
- (40) Wu, K.; Lian, T. Quantum Confined Colloidal Nanorod Heterostructures for Solar-to-Fuel Conversion. *Chem. Soc. Rev.* **2016**, 45, 3781–3810.
- (41) Klimov, V. I.; Mikhailovsky, A. A.; McBranch, D. W.; Leatherdale, C. A.; Bawendi, M. G. Quantization of Multiparticle Auger Rates in Semiconductor Quantum Dots. *Science* **2000**, 287, 1011–1013.
- (42) Klimov, V. I. Spectral and Dynamical Properties of Multi-excitons in Semiconductor Nanocrystals. *Annu. Rev. Phys. Chem.* **2007**, 58, 635–673.
- (43) Robel, I.; Gresback, R.; Kortshagen, U.; Schaller, R. D.; Klimov, V. I. Universal Size-Dependent Trend in Auger Recombination in Direct-Gap and Indirect-Gap Semiconductor Nanocrystals. *Phys. Rev. Lett.* 2009, 102, 177404.

- (44) Klimov, V.; Bolivar, P. H.; Kurz, H. Ultrafast Carrier Dynamics in Semiconductor Quantum Dots. *Phys. Rev. B: Condens. Matter Mater. Phys.* **1996**, *53*, 1463–1467.
- (45) Klimov, V. I.; Schwarz, C. J.; McBranch, D. W.; Leatherdale, C. A.; Bawendi, M. G. Ultrafast Dynamics of Inter- and Intraband Transitions in Semiconductor Nanocrystals: Implications for Quantum-Dot Lasers. *Phys. Rev. B: Condens. Matter Mater. Phys.* 1999, 60, R2177–R2180.
- (46) Klimov, V. I. Optical Nonlinearities and Ultrafast Carrier Dynamics in Semiconductor Nanocrystals. *J. Phys. Chem. B* **2000**, *104*, 6112–6123.
- (47) Zhu, H.; Yang, Y.; Wu, K.; Lian, T. Charge Transfer Dynamics from Photoexcited Semiconductor Quantum Dots. *Annu. Rev. Phys. Chem.* **2016**, *67*, 259–281.
- (48) Klimov, V. I. Spectral and Dynamical Properties of Multi-lexcitons in Semiconductor Nanocrystals. *Annu. Rev. Phys. Chem.* **2007**, *58*, 635–673.
- (49) Huang, J.; Stockwell, D.; Huang, Z. Q.; Mohler, D. L.; Lian, T. Q. Photoinduced Ultrafast Electron Transfer from CdSe Quantum Dots to Re-Bipyridyl Complexes. *J. Am. Chem. Soc.* **2008**, *130*, 5632–5633
- (50) Morris-Cohen, A. J.; Frederick, M. T.; Cass, L. C.; Weiss, E. A. Simultaneous Determination of the Adsorption Constant and the Photoinduced Electron Transfer Rate for a CdS Quantum Dot–Viologen Complex. *J. Am. Chem. Soc.* **2011**, *133*, 10146–10154.
- (51) Grimaldi, G.; Geuchies, J. J.; van der Stam, W.; du Fossé, I.; Brynjarsson, B.; Kirkwood, N.; Kinge, S.; Siebbeles, L. D. A.; Houtepen, A. J. Spectroscopic Evidence for the Contribution of Holes to the Bleach of Cd-Chalcogenide Quantum Dots. *Nano Lett.* **2019**, 19, 3002–3010.
- (52) Kunneman, L. T.; Schins, J. M.; Pedetti, S.; Heuclin, H.; Grozema, F. C.; Houtepen, A. J.; Dubertret, B.; Siebbeles, L. D. A. Nature and Decay Pathways of Photoexcited States in CdSe and CdSe/CdS Nanoplatelets. *Nano Lett.* **2014**, *14*, 7039–7045.
- (53) Cassette, E.; Pedetti, S.; Mahler, B.; Ithurria, s.; Dubertret, B.; Scholes, G. Ultrafast Exciton Dynamics in 2D In-Plane Hetero-Nanostructures: Delocalization and Charge Transfer. *Phys. Chem. Chem. Phys.* **2017**, *19*, 8373–8379.
- (54) Morgan, D. P.; Maddux, C. J. A.; Kelley, D. F. Transient Absorption Spectroscopy of CdSe Nanoplatelets. *J. Phys. Chem. C* **2018**, *122*, 23772–23779.
- (55) Li, Q.; Lian, T. Ultrafast Charge Separation in Two-Dimensional CsPbBr₃ Perovskite Nanoplatelets. *J. Phys. Chem. Lett.* **2019**, *10*, 566–573.
- (56) Mahler, B.; Nadal, B.; Bouet, C.; Patriarche, G.; Dubertret, B. Core/Shell Colloidal Semiconductor Nanoplatelets. *J. Am. Chem. Soc.* **2012**, *134*, 18591–18598.
- (57) Dong, S.; Pal, S.; Lian, J.; Chan, Y.; Prezhdo, O. V.; Loh, Z.-H. Sub-Picosecond Auger-Mediated Hole-Trapping Dynamics in Colloidal CdSe/CdS Core/Shell Nanoplatelets. *ACS Nano* **2016**, *10*, 9370–9378
- (58) Singh, S.; Tomar, R.; ten Brinck, S.; De Roo, J.; Geiregat, P.; Martins, J. C.; Infante, I.; Hens, Z. Colloidal CdSe Nanoplatelets, a Model for Surface Chemistry/Optoelectronic Property Relations in Semiconductor Nanocrystals. *J. Am. Chem. Soc.* **2018**, *140*, 13292–13200
- (59) Feldmann, J.; Peter, G.; Gobel, E. O.; Dawson, P.; Moore, K.; Foxon, C.; Elliott, R. J. Linewidth Dependence of Radiative Exciton Lifetimes in Quantum-Wells. *Phys. Rev. Lett.* **1987**, *59*, 2337–2340.
- (60) Bird, C. L.; Kuhn, A. T. Electrochemistry of the Viologens. Chem. Soc. Rev. 1981, 10, 49–82.
- (61) Zhu, H.; Yang, Y.; Hyeon-Deuk, K.; Califano, M.; Song, N.; Wang, Y.; Zhang, W.; Prezhdo, O. V.; Lian, T. Auger-Assisted Electron Transfer from Photoexcited Semiconductor Quantum Dots. *Nano Lett.* **2014**, *14*, 1263–1269.
- (62) Diroll, B. T.; Fedin, I.; Darancet, P.; Talapin, D. V.; Schaller, R. D. Surface-Area-Dependent Electron Transfer between Isoenergetic 2D Quantum Wells and a Molecular Acceptor. *J. Am. Chem. Soc.* **2016**, 138, 11109–11112.

- (63) Okuhata, T.; Tamai, N. Face-Dependent Electron Transfer in CdSe Nanoplatelet–Methyl Viologen Complexes. *J. Phys. Chem. C* **2016**, *120*, 17052–17059.
- (64) Wu, K.; Du, Y.; Tang, H.; Chen, Z.; Lian, T. Efficient Extraction of Trapped Holes from Colloidal CdS Nanorods. *J. Am. Chem. Soc.* **2015**, *137*, 10224–10230.
- (65) Shinada, M.; Sugano, S. Interband Optical Transitions in Extremely Anisotropic Semiconductors. I. Bound and Unbound Exciton Absorption. J. Phys. Soc. Jpn. 1966, 21, 1936–1946.
- (66) Schmitt-Rink, S.; Chemla, D. S.; Miller, D. A. B. Theory of Transient Excitonic Optical Nonlinearities in Semiconductor Quantum-Well Structures. *Phys. Rev. B: Condens. Matter Mater. Phys.* **1985**, 32, 6601–6609.
- (67) Chernikov, A.; Berkelbach, T. C.; Hill, H. M.; Rigosi, A.; Li, Y.; Aslan, O. B.; Reichman, D. R.; Hybertsen, M. S.; Heinz, T. F. Exciton Binding Energy and Nonhydrogenic Rydberg Series in Monolayer WS₂. *Phys. Rev. Lett.* **2014**, *113*, 076802.
- (68) Hill, H. M.; Rigosi, A. F.; Roquelet, C.; Chernikov, A.; Berkelbach, T. C.; Reichman, D. R.; Hybertsen, M. S.; Brus, L. E.; Heinz, T. F. Observation of Excitonic Rydberg States in Monolayer MoS₂ and WS₂ by Photoluminescence Excitation Spectroscopy. *Nano Lett.* **2015**, *15*, 2992–2997.
- (69) Benchamekh, R.; Gippius, N. A.; Even, J.; Nestoklon, M. O.; Jancu, J. M.; Ithurria, S.; Dubertret, B.; Efros, A. L.; Voisin, P. Tight-Binding Calculations of Image-Charge Effects in Colloidal Nanoscale Platelets of CdSe. *Phys. Rev. B: Condens. Matter Mater. Phys.* **2014**, 89, 035307.
- (70) Wannier, G. H. The Structure of Electronic Excitation Levels in Insulating Crystals. *Phys. Rev.* **1937**, *52*, 191–197.
- (71) Elliott, R. J. Intensity of Optical Absorption by Excitons. *Phys. Rev.* **1957**, *108*, 1384–1389.
- (72) Li, Z.; Qin, H.; Guzun, D.; Benamara, M.; Salamo, G.; Peng, X. Uniform Thickness and Colloidal-Stable CdS Quantum Disks with Tunable Thickness: Synthesis and Properties. *Nano Res.* **2012**, *5*, 337–351.